Functional Ecology

BRITISH ECOLOGICAL SOCIETY

Change in drivers of mangrove crown displacement along a salinity stress gradient

Journal:	*Functional Ecology*
Manuscript ID	FE-2018-00734.R1
Manuscript Type:	Research Article
Date Submitted by the Author:	18-Aug-2018
Complete List of Authors:	Vovides, Alejandra; University of Glasgow, School of Geographical and Earth Sciences; Instituto de Ecologia, Functional Ecology Network Berger, Uta; Dresden University of Technology, Department of Forest Sciences Grueters, Uwe; Dresden University of Technology, Department of Forest Sciences Guevara, Roger; Instituto de Ecologia A.C., Carretera antigua a Coatepec 351,, El Haya Pommerening, Arne; Swedish University of Agricultural Sciences, Department of Forest Resource Management Lara-Domínguez, Ana; Instituto de Ecologia, Functional Ecology Network Lopez Portillo, Jorge; Instituto de Ecologia
Key-words:	Avicennia germinans, crown displacement, mangroves, neighbourhood avoidance, above-ground interactions, Rhizophora mangle, salinity stress gradient, wind direction

Note: The following files were submitted by the author for peer review, but cannot be converted to PDF. You must view these files (e.g. movies) online.

Fig 1.png

Change in drivers of mangrove crown displacement along a salinity stress gradient

Alejandra G. Vovides[1,2], Uta Berger[3], Uwe Grueters[3], Roger Guevara[4], Arne Pommerening[5], Ana Laura Lara-Domínguez[1], Jorge López-Portillo[1]

[1]Functional Ecology Network, Instituto de Ecología A.C. Xalapa, Veracruz, Mexico

[2]School of Geographical and Earth Sciences, University of Glasgow, United Kingdom

[3]Department of Forest Biometry and Systems Analysis, Institute of Forest Growth and Forest Computer Sciences, Technische Universität Dresden, Tharandt, Germany

[4]Evolutionary Biology Network, Instituto de Ecología A.C. Xalapa, Veracruz, Mexico

[5]Department of Forest Resource Management, Faculty of Forest Sciences, Swedish University of Agricultural Sciences, Umeå, Sweden

Correspondence

Dr. Alejandra G. Vovides

Alejandra.Vovides@glasgow.ac.uk

Running title: Effect of neighbours and wind on mangrove crown displacement along a salinity gradient

Abstract

1. Crown displacement in trees is an adaptive response driven by neighbours that optimizes space use and reduces competition. But it can also be the result of wind forces. Although morphological responses to neighbours have been well studied, the interplay between neighbours and wind as drivers of crown shape, and its implications for plant interactions remains poorly understood, and it is relevant to predict changes in vegetation structure and function under the scope of global change. We test the hypothesis that above-ground interactions are reduced with increasing soil stress and that wind becomes the main driver of crown shape in mangrove forests.
2. We investigated the effect of neighbours and wind intensity and direction on crown displacement of mangrove canopy and below canopy trees along a salinity gradient, and assessed crown asymmetry for three mangrove tree species, as well as the contribution of crown displacement on reducing crown projected area overlap and thus neighbourhood competition.
3. Results show that crown displacement of canopy trees is strongly influenced by winds at all salinities. At low salinities, competition for space accounted for 48% of crown displacement away from neighbours, compared to 49% found with the synthetized effects of wind and neighbours. While trees below the canopy displace their crowns away from their neighbours, and no response to wind could be detected. This can be due to the wind protection conferred by a dense canopy stand related to bigger crowns that effectively reduce wind drag. At higher salinities, there was a reduction in canopy overlap due to crown displacement, which suggests reduced above-ground plant interactions with increasing soil stress.

4. While neighbourhood avoidance is a fundamental strategy for optimal light foraging, this study shows that wind strength and directionality are main drivers of crown shape with increasing stress, and highlights their potential influence in plant interactions and forest structure, pointing to an increased susceptibility of trees to disturbances that should be further studied.

Keywords: *Avicennia germinans,* crown displacement, mangroves, neighbourhood avoidance, above-ground interactions, *Rhizophora mangle*, salinity stress gradient, wind direction.

Introduction

Tree-crown responses to neighbours have attracted the interest of forestry and ecology scholars to understand mechanisms of species interaction and coexistence (Brisson, 2001; Brooker, 2006; Jucker, Bouriaud, & Coomes, 2015; Longuetaud, Piboule, Wernsdörfer, & Collet, 2013). The modular growth of plants allows for the directional allocation of plant biomass toward resource-rich areas, optimizing foraging and, in many instances, reducing competition among neighbours (Brisson, 2001; Brisson & Reynolds, 1994; Longuetaud et al., 2013). However, tree crowns can also be shaped by wind (MacFarlane & Kane, 2017; Telewski & Jaffe, 1986), creating an asymmetry similar to that resulting from the active growth of the tree in response to neighbours.

Tree morphological responses to environmental cues can be reflected in the whole tree architecture and in the crown shape; under crowding conditions, trees have spindly stem and dispersedly distributed slender branches that improve light foraging, while solitary trees possess a wind-resistant architecture, with increased radial growth and reduced elongation of stem, branches and leaves (MacFarlane & Kane, 2017; Telewski, 2006). Several studies associate greater crown displacements (distance between the crown centroid and the stem base, Brisson, 2001) with decreasing distances to neighbouring trees and species-specific attributes such as higher light-demand (Longuetaud et al., 2013; Longuetaud, Seifert, Leban, & Pretzsch, 2008; Schröter, Härdtle, & Oheimb, 2011). Since crown displacement reduces competition for light and may increase individual fitness, it can be considered an active trait resulting from a growth response to light availability (Longuetaud et al., 2013; Vacchiano, Castagneri, Meloni, Lingua, & Motta, 2011). On the other hand, elongated crowns with their narrow sides parallel to the wind direction can reduce wind drag (Telewski, 2006; Telewski & Jaffe, 1986), reducing the risk of mechanical failure. In this case, crown morphology may result from branch damage due to wind

and crown collisions and is reflected in the direction of displacement (Rudnicki, Silins, & Lieffers, 2004; Rudnicki, Silins, Lieffers, & Josi, 2001; Uria-Diez & Pommerening, 2017), or in response to the mechanical pressure exerted by wind, which can inhibit branch elongation (Rudnicki et al., 2001; Telewski, 2006; Telewski & Jaffe, 1986).

The relevance of wind and neighbours on plant interactions along stress gradients, especially for tropical plant communities, is not well understood but should be relevant to conservation and management. Limiting soil conditions can also trigger differential biomass allocation patterns, shifting from above- to below- ground competition (Tilman, 1990), causing variation in morphological traits along environmental stress gradients (Schöb, Armas, Guler, Prieto, & Pugnaire, 2013; Vovides et al., 2014). Yet, the interplay between wind and neighbours in shaping tree interactions remains unclear, although it could be an effective approach to understand spatial trait variation and drivers of community structure with environmental heterogeneity and global change. This work disentangles the contribution of these two factors along a soil stress gradient within a mangrove forest in the central Gulf Coast of Mexico.

Mangrove forests are suitable for this study since they grow in flat terrains, and along a wide range of soil salinity, thus slopes and light directionality should have little effect on crown shape. Mangrove plastic responses to saline stress are remarkable. At individual level, trees become smaller and with wider stems in relation to height, allowing trees to maintain an optimal water balance at higher salinities (Robert, Koedam, Beeckman, & Schmitz, 2009; Vovides et al., 2014), and at stand level, size-asymmetry is reduced, potentially reducing above-ground competition (Méndez-Alonzo, Hernández-Trejo, & López-Portillo, 2012; Naidoo, 2009). Additionally, seasonal north trade winds with speeds up to 28 m s^{-1} dominate during seven months of the year (end of September to early May). While regular strong winds are known to

restrict tree height and cause asymmetric crowns, increasing mechanical stability and reducing wind dynamic loading (Holtmeier & Broll, 2010; Telewski & Jaffe, 1986), a better understanding of the role of wind in modulating plant interactions is needed to predict outcomes of increasing storm frequencies and sea level rise on ecosystems structure and function (Easterling et al., 2000; Krauss et al., 2014; Woodroffe, 1990). Since soil stress is expected to reduce aboveground competition (Emery, Ewanchuk, & Bertness, 2001; Tilman, 1988, 1990), in this study we test the hypothesis that with increasing salinity, aboveground interactions are reduced, and wind becomes a major driver of crown displacement. Focusing on the combined effects of neighbours and wind direction on crown displacement on different mangrove species, we hypothesise that shade tolerant species will show more symmetric crowns, and less displacement responses to neighbour shading in relation to light demanding species. To test these hypothesis, we associated crown displacement to a trees' neighbourhood asymmetry (defined as a vector that reflects the location and size of neighbours, Brisson, 2001), and wind direction for trees growing at and below the canopy, since below canopy trees are protected from wind and thus wind should have less effect on their crown shapes. We evaluated the magnitude of crown asymmetry for three mangrove species, and its contribution to the reduction of crown overlap along a salinity gradient ranging between 4.6 and 60 ppt within two neighbouring environmental settings.

Materials and methods

STUDY AREA

This study was conducted in the mangroves of the La Mancha Lagoon (19°35'N, 96°22'W) in the state of Veracruz, Mexico (Fig. 1). The mean annual temperature in the area is 25°C and the

mean annual precipitation is 1200 mm (Méndez-Alonzo, Hernández-Trejo, et al., 2012). The lagoon communicates in its northernmost side with the Gulf of Mexico through an ephemeral inlet that closes between October and April, during the north trade wind season, while a permanent fresh water stream imports water to the lagoon to its southernmost side throughout the year (Psuty et al., 2009). This hydrology contributes to a salinity gradient that increases from the southernmost point of the lagoon to its northernmost side, influencing the structure of the mangrove forest (Fig. 1), except for a small area in the north of the lagoon (IB1), where salinity is below five ppt due to the influence of a neighbouring flooded grassland (Moreno-Casasola et al., 2009).

From a geomorphological point of view, two contrasting habitats predominate in the mangrove forest: mudflats (MF) and Interdistributary basins (IB). In the MFs, the water table decreases during the dry season, resulting in fine clay deposits and increased salt accumulation, succeeded by periodic tidal flooding and runoff of fresh water during the rainy season that can lower salinity levels. The IBs flank the main waterways that drain fresh water from higher lands towards the lagoon, contributing to high accumulation of organic matter and keeping low salinity throughout the year (Méndez-Alonzo, Pineda-García, Paz, Rosell, & Olson, 2012). Mean height of top-height trees (20% of highest trees in the stand) is 14.65 m for IB and 12.7 m for MFs, trees in IB environments are more slender (D_{130}/H), having stems 20% narrower and crown areas 10% narrower than in MF (Vovides et al., 2014).

DATA COLLECTION

A total of 12 permanent study plots (10 with 30 m x 30 m, and two with higher density were 20 m x 20 m) were traced with a north-south orientation and located at similar distance from the

closest main water body (Figure 1). Six of them were located within IB, and six in MF mangrove habitats following the salinity gradient. In all plots, trees with stem diameters >2.5 cm were tagged. A Haglöf electronic clinometer and ultrasonic meter (Långsele, Sweden) and a Suunto compass (Vantaa, Finland) were used to measure the distance (d) and angle (θ) of each tree stem from the centre of the plot, to further compute each tree stem_i Cartesian position $\begin{pmatrix} S_{x_i} = d_i \cos\theta_i \\ S_{y_i} = d_i \sin\theta_i \end{pmatrix}$ within the plot. Pore-water salinity was measured in three samples of soil pore-water at 20 cm depth, during the dry season (end of November to mid-May) of 2011 and at the end of the rainy season (end of May to mid-November) of 2014, using a pore-water extractor as described by McKee et al. (1988). Soil pore-water was then placed in a Myron L Ultrameter II conductivity measuring device (Carlsbad, Canada). Averaged salinity data from the wet and dry seasons were used as salinity values influencing each plot throughout the year.

Tree species, density (trees ha^{-1}), height (H, m) and stem diameters at a 130 cm above ground level (D_{130}, cm) were recorded using the ultrasonic meter and a 100 cm Haglöf calliper (Långsele, Sweden). To measure crown radii, the compass and a GRS densitometer (Arcata, California, United States) were used to locate the edge of the crown in eight cardinal directions (E, NE, …SE) and the Vertex III range meter was used to measure the distance between basal stem position and the edge of the crown projected to the ground. The resulting eight radii were further used to reconstruct crown-projected areas.

Wind speeds and direction measurements taken every 10 minutes for the years 2011-2014 were obtained from the National Oceanic and Atmospheric Administration's meteorological station LMBV4 (NOAA, 2016), located within 3.2 km from the study plots. Annual mean wind speeds and direction for these years averaged 3 m s^{-1} and 33° Northeast, respectively, while the average wind speed for winds >4 m s^{-1} is 5.6 m s^{-1} with a mean direction of 47° Northeast, and

maximum wind speed reached 20 m s^{-1}, with 27° NW direction. Winds above 4 m s^{-1} were chosen as they represent the minimum speed that can cause crown tilting, collisions and thus, canopy damage (Rudnicki et al., 2001).

From the collected data, we calculated basal area (m^2 ha^{-1}), relative density (%), and species relative dominance (%). For each $tree_i$, we computed the crown-projected polygon area (A_i), defined as the sum of the areas of eight triangles that result from the distance between stem position and crown projected border measured in eight cardinal directions

$$A_i = \frac{1}{2}(x_{c,1}y_{c,2} - x_{c,2}y_{c,1}) + \cdots + \frac{1}{2}(x_{c,7}y_{c,8} - x_{c,8}y_{c,7}) + \frac{1}{2}(x_{c,8}y_{c,1} - x_{c,1}y_{c,8}),$$

the position of the projected crown polygon centroid (G_i), as the centre of mass of the polygon (Fig 2A), and the vector of crown displacement (u_i), defined as the vector between stem base position (S_i) and G_i (Fig. 2A). These parameters were further used to study crown responses to neighbour location and wind direction as described in the following sections.

CROWN DISPLACEMENT AND NEIGHBOURHOOD ASYMMETRY

To evaluate the response of tree crowns to neighbourhood pressure, a vector of asymmetric neighbourhood (v_i, Fig. 2A) was computed, reflecting the direction and magnitude of pressure from neighbouring trees to a focal tree expressed as:

$$v_i = \sum_j \frac{A_j}{|S_j - S_i|^2}(S_j - S_i),$$

Where the sum runs over the neighbours j of $tree_i$. A_j is the projected crown polygon area of each neighbour. $|S_j - S_i|$ denotes the magnitude of a vector between focal $tree_i$ stem position and neighbours' j stem position (Brisson, 2001; Brisson & Reynolds, 1994), and the vector itself is expressed as $(S_j - S_i)$. Thus, weights in the computation of v_i represent the neighbors' crown areas divided by the squared distance of their stem position from the stem position of the focal

tree S_i. Here and below, the term "neighbour" refers to all trees located ≤ 5 m from the focal tree. The five-meter radius neighbourhood ensured our analysis accounted for the most crucial neighbour effects, leaving enough trees with complete neighbourhoods within the plots.

To evaluate if crown displacement is a response to a trees' asymmetric neighbourhood, we computed for each tree, the alignment (a_i, Fig. 2B) between direction of neighbourhood pressure (v_i) and direction of crown displacement (u_i) as the dot product of v_i and u_i divided by the length of v_i:

$$a_i = u_i \cdot \frac{v_i}{|v_i|} = \frac{v_{i,1}u_{i,1}+v_{i,2}u_{i,2}}{|v_i|}.$$

The dot product is a mathematical expression that applies the directional growth of one vector to another vector (Matthews, 2000). a_i is thus, the projection of u_i along the direction of v_i (Fig. 2B). If a_i is positive, crowns are shifted towards their neighbours, while negative values indicate that crowns are shifted away from their neighbours. Due to the low number of *L. racemosa* trees in the studied plots, changes on alignment along the salinity gradient were evaluated using a generalized mixed effects model with a Markov chain Monte Carlo algorithm (MCMC) that allowed to model responses of all species through a resampling chain of 13,000 iterations, 3,000 burn-in iteration rounds, and a ten-fold thinning. Thus, 1,000 samples were retained, specifying salinity and species as fixed effects and habitat as a random effect.

CONTRIBUTION OF CROWN ASYMMETRY TO THE REDUCTION OF CROWN OVERLAP

To evaluate for reduction in crown asymmetry along the salinity gradient, we computed an index of crown asymmetry (D_b), a unitless measure developed by Brisson (2001) to assess the

magnitude of crown displacement from the tree stem base, omitting possible effects of tree size on crown asymmetry.

$$D_b = \frac{|u_i|}{\omega_i}$$

Where $|u_i|$ is the length of the vector of crown displacement, and ω_i is the weighted mean distance of all vertices of the crown polygon from G_i (see Brisson, 2001 for details on the calculation of ω_i). A D_b = 0 indicates a perfectly symmetric crown, with its centroid located over the stem; $D_b = 1$, indicates the crown boundary is located above the stem base. Variations in D_b were evaluated between habitats, species, and tree height using a generalized additive mixed effect model with species and salinity as fixed effects, tree height as a smoothing term, and habitat as random effects. Tree height was chosen as smoothing term to evaluate for non-linear patterns of crown asymmetry along tree height, implementing a spline function available for GAM models in the R package "mgvc".

To estimate crown projected area overlap in each plot, we mapped the crown polygons and computed the total canopy cover (area covered by at least one crown) and the total overlapping area (area covered by at least two overlapping crowns). Because the area of two sampling plots differed from the rest, and also because crown diameters decrease with increasing salinities (Vovides et al., 2014), we calculated relative canopy cover (%) and relative crown overlap (%) with the observed asymmetry and crown displacement (O_{crown} in %). Further, u_i was used to virtually place crown centroids (G_i) over the basal stem positions (S_i), and the resulting mapped overlapped areas were quantified (O_{stem}, Fig. 2D). We also used A_i to simulate regular octagons and estimate relative overlap assuming symmetric and centred crowns (O_{symm}, Fig. 2E). Crown polygon maps were computed in R version 3.4.3, and image analysis was performed using the

GIMP V2.8 image analysis package. See Appendix S1 in supporting information for details on the computation of regular octagons.

Overlap reduction due to crown displacement and asymmetry were then computed as: 1) the difference in relative crown overlap between crowns centred in S_i and crowns with centred in G_i ($\Delta O_{displacement} = O_{stem} - O_{crown}$), and 2) the difference between overlap of symmetric centred crowns centred S_i and the overlap as observed in the field ($\Delta O_{symm} = O_{symm} - O_{crown}$).

When assessing the contribution of crown displacement to the reduction of crown overlap, and due to the reduction on relative canopy cover along the salinity gradient, a best fit linear mixed effects model was selected by the maximum likelihood approach using the Akaike Information Criterion. We started all analyses with a null model that included salinity, relative canopy cover and density as fixed effects and habitat as random effect. Stepwise we extracted predictor variables to evaluate whether the model was improved until only the fixed effect variable salinity and random effect habitat were left.

DIRECTIONALITY OF CROWN DISPLACEMENT

To study the direction of crown displacement as a response to neighbours and wind, the angles of u_i were further evaluated by means of the Rayleigh test, a circular statistics approach that assesses the aggregation of data points around the circle. With this test, the sample mean resultant length (ρ) is computed as a measure of how the data are distributed around a circular plane (Pewsey, Neuhäuser, & Ruxton, 2013). When all data points are located at the same angle in the circle ρ = 1, values close to one indicate that data points are aggregated around a mean

direction, while values close to cero indicate that points are spread evenly around the circle (Pewsey et al., 2013).

Additionally, to study the pressure exerted by neighbours and wind on crown displacement, a wind vector was added to v_i:

$$nw_i = v_i + f\overrightarrow{NE},$$

where f is wind speed. Values used for f were 20 m s^{-1} (max. wind seed) and 5.6 m s^{-1} (the mean for all events greater >4 m s^{-1} between the years 2011 and 2014), $\overrightarrow{NE}$ is the direction of the wind vector, set at 40° northeast for the mean wind seed, and 117° degrees for maximum wind speed direction (when east = 0 and rotation is counter clockwise).

Further, we computed the angles of alignment (φ; Fig. 2B) between u_i and v_i (φ_v, for the effect of neighbourhood asymmetry), u_i and $\overrightarrow{fNE}$ (φ_w, for the effect of wind), and u_i and nw_i (φ_{nw}, for the effect of neighbourhood asymmetry and wind). If the resulting φ is close to 180°, u_i opposes the v_i, and focal tree crowns are displaced away from the direction of pressure. The Rayleigh tests were performed separately for trees below the canopy and for canopy trees, and 95% confidence intervals were estimated by a bootstrap for a von Misses distribution on 1,000 iterations. Given that allometric relations change between the two habitats (Vovides et al., 2014), the average height of top-height trees from each habitat was taken as splitting point to separate canopy and below-canopy trees:13 m for MF and 15 m IB, to ensure the responses of below canopy trees are not confounded with dominant trees at the canopy level.

All vector computations, polygon mapping and statistical analyses were performed using R V 3.2.3 (R Core Team, 2015). Specific packages include: 1) “nmle”, “MASS”, “mgvc”, “car” and “MCMCglmm” for generalized mixed effects models and generalized additive mixed effects

models, 2) packages "circular", "CircStat" and "CircLME" for circular analyses (Agostinelli & Lund, 2013).

Results

Soil salinity ranged from 4.6 ± 0.54 to 60.40 ± 2.52 ppt (mean ± se). The lowest salinity was found in plot IB1, and the highest at plot MF6 (Figure 1). *A. germinans* was the dominant species in most sites, except in IB1 and IB2. Despite being an abundant species in IB1, *A. germinans* individuals had a basal area 38% smaller than that of *L. racemosa* (Table 1). Plots located in Interdistributary basins were mixed forests co-dominated by *L. racemosa* and *A. germinans* (plot IB1) or by *R. mangle* and *A. germinans* (IB2 and IB6), while mudflats were predominantly monospecific *A. germinans* forests (Table 1).

CROWN DISPLACEMENT AND NEIGHBOURHOOD AVOIDANCE

The MCMC generalized mixed effects model applied to assess the alignment a_i between v_i and u_i showed a significant reduction on the contribution of neighbours to crown displacement along the salinity gradient (pMCMC = 0.02), as negative values become smaller and positive values of a_i increase for all species (pMCMC = 0.01, 0.05, and 0.01, for *A. germinans*, *L. racemosa* and *R. mangle*, respectively, Fig. 3). The species with greater negative values of a_i was *A. germinans*, with negative mean alignments for the posterior density probabilities, while they lay towards positive values for *R. mangle* and *L. racemosa* (Fig. 4).

Within IBs, *A. germinans* canopy tree crowns were significantly displaced on a SW direction with (mean direction at 207^o ± 29^o, confidence intervals at 95%), when 0^o = E and rotation is counter clock wise, (ρ = 0.33, P = 0.006, Fig. 5A), while there was no significant

direction of displacement for tree crowns below the canopy (ρ = 0.13, P = 0.19, Fig. 5A). In MF habitats, the crowns of canopy and below canopy trees (Fig. 5C), were displaced towards SW direction (203 ± 44°, ρ = 0.19, P = 0.03, and 207 ± 26°, ρ = 0.21, P = 0.003, respectively). For *R. mangle*, only below canopy crowns at IB had a significant crown displacement towards S-SW (254 ± 26°, ρ = 0.22, P = 0.004).

When using maximum wind speed and direction to assess the alignment between the crown direction and the vector of pressure, the mean angle of alignment φ_{nw} varied between 90° and 113° for *A. germinans* for both habitats at- and below canopy level, with the highest concentration parameter found for canopy trees in the IB ($\rho = 0.35, P < 0.005$), at a mean angle of 104°, which is inconsistent with the expected mean direction (close to 180°) for crowns displaced away from the direction of pressure. For *R. mangle*, the use of maximum wind speed in the analyses returned very similar results to those involving the mean wind speed and direction, and therefore, we will present only the results for mean wind speed and directions for both species.

Within IBs, the estimated angles of alignment (φ_v, φ_w and φ_{nw}) for *A. germinans* canopy trees are significantly aggregated around a mean direction of 173° (Table 2, Figs. 6A and 6B), with the highest concentration parameter corresponding to the combined effect of neighbours and wind (φ_{nw}, $\rho = 0.49, P =< 0.0001$, Table 2). Crown directionality below the canopy showed significant aggregation towards 168° for φ_v, while wind and the combined effect of wind and neighbours did not show a significant alignment (Table 2, and Fig. 6A). For *R. mangle* in IBs, significant aggregation was found for φ_{nw} both at canopy and below canopy levels and for below canopy trees when considering only wind (for φ_w) in the vector of pressure (Table 2 and Figs. 6C and 6D). In MFs, for *R. mangle*, and *A. germinans* the highest

326 concentration parameters were obtained when including the effect of neighbours and wind (φ_{nw},
327 Table 2 and Figs. 6E-6H), with close to double the aggregation of data points around a mean
328 direction of 171° than the observed for vectors of pressure including only wind or only
329 neighbours (Table 2).
330
331 CROWN DISPLACEMENT AND REDUCTION OF CROWN OVERLAP
332 D_b was greater in IB than in MF habitats (P = 0.04), but did not change significantly along the
333 salinity gradient (P = 0.8). Differences in D_b between species were significant (P < 0.01); the
334 highest D_b was recorded for the species *L. racemosa* (0.76 ± 0.03, mean ± se) and the lowest was
335 recorded for *R. mangle* in MF plots (0.33 ± 0.04), while *A. germinans* had a mean D_b of 0.63 ±
336 0.02 in MF and 67 ± 0.02 in IB. The model's smooth term (tree height) showed the highest D_b at
337 tree heights between 5 and 10 m (P < 0.001, df = 2.5), and decreased as tree height increased
338 (Fig. 7).
339 Relative canopy cover ranged from 44% in MF5 to 97% in IB3, and relative crown
340 overlap ranged from 5% in MF3 to 55% in IB1. Although a significant reduction on relative
341 canopy cover was detected along the salinity gradient (b = -0.87, se = 0.23, t-value = -3.73, P =
342 0.005), this did not explain the reduction in canopy overlap with increasing salinity. The best fit
343 models to explain the reduction of relative canopy overlap for $\Delta O_{stem-crown}$ and $\Delta O_{symm-crown}$,
344 included only relative salinity as fixed effects and habitat as random effect. For $\Delta O_{stem-crown}$,
345 crown displacement reduced crown overlap up to 15% at the lowest salinity (Intercept = 15.52%,
346 b= -0.24, t= -8.07, Fig. 8). When using absolute symmetric crowns ($\Delta O_{symm-crown}$) overlap was
347 reduced up to 39% at 25 ppt (Intercept = 35.48, b = -0.53, t= -3.7, Fig. 8).
348

Discussion

Our results support the hypothesis of a change in drivers of crown shape with increased soil stress. We found strong evidence of reduced above ground inter-plant interactions and a shift from crown displacement driven by neighbour size and location to crowns shaped by wind forces as soil salinity increases. These findings are consistent with the resource competition theory in that above ground competition decreases as abiotic environmental stress increases (Tilman, 1988, 1990). The aim of this work was not to test the theory in terms of resource allocation patterns and the shift towards belowground competition. We rather focused on the interplay between neighbours and wind speed and direction as drivers of crown asymmetry and patterns of aboveground interaction in a setting of increasing soil environmental stress.

The strength of competition between two trees can be defined by their size and the distance between each other, larger trees will have higher zones of influence, and the closer they are to a neighbour, the stronger the competition will be (Berger & Hildenbrandt, 2000). Thus, the ability to shift crowns away from the most competitive neighbours, increases the distance between trees, optimizing space use and reducing competitive interactions. This finding is consistent with other studies developed in temperate forests, describing crown displacement as an adaptive strategy towards optimal light foraging and competition avoidance (Aakala, Shimatani, Abe, Kubota, & Kuuluvainen, 2016; Brisson, 2001; Longuetaud et al., 2013; Uria-Diez & Pommerening, 2017; Wolf, Field, & Berry, 2011), and is supported by the reduced ΔO at increasing salinities, evidence of reduced above-ground interactions. But the response to local neighbourhoods gradually reduces with increasing salinity, yet crowns show asymmetric shapes, and this was related to wind forces.

371 The observed directionality of crown displacement towards SW and angles of alignment
372 best explained by the synthesised effect of wind and neighbours, points to a greater influence of
373 wind directionality on crown displacement in higher salinities, and suggests an increased
374 susceptibility to wind dynamic loading, presumably as a consequence of salinity-induced
375 reduction in growth rate (Ball, 1988; Nguyen, Stanton, Schmitz, Farquhar, & Ball, 2015). This is
376 ultimately expressed in smaller canopies (Vovides et al., 2014) with lower wind damping (James,
377 Haritos, & Ades, 2006; MacFarlane & Kane, 2017). Within MF, the observed reduced canopy
378 cover and reduced crown overlap related to smaller trees, could explain the greater effect of wind
379 at higher salinities; smaller tree sizes and crowns could render greater canopy openness. Thus,
380 higher wind speeds in the vertical scale of the forest would have greater influence in crown
381 displacement, as found for edge trees and for open-grown trees vs crowded trees in temperate
382 forests (Brüchert & Gardiner, 2006; MacFarlane & Kane, 2017). However, the reduced crown
383 displacements away from neighbours at higher salinities, showed by the MCMCglm, could
384 represent an advantage in terms of wind protection. More aggregated crowns could help reduce
385 wind dynamic loading, since wind movement is limited by neighbour proximity (Nicoll & Ray,
386 1996). This would not only effectively reduce wind loading on crowns, but could also increase
387 the frequency of crown collisions during wind events, creating branch damage, and prompt
388 crown shyness, exerting greater influence on crown asymmetry than active growth towards light
389 would (Rudnicki et al., 2004, 2001).

390 The observed patterns on the direction of crown displacement also reveal the influence of
391 prolonged exposure to north-trade winds, supporting the findings by Rudnicki et al. (2001) that
392 wind speeds between 4 and 10 m s^{-1} can create a frequency of collisions that contributes to
393 crown asymmetry and can inhibit lateral shoot extension (Telewski, 2006). These results are also

consistent with the observations that plants are sensitive to perturbation frequency rather than to the magnitude of pressure exerted on them (Telewski, 2006), which would explain the mean angles of alignment closer to 180° for φ_{nw} when assessing mean (5.6 m s^{-1}) wind speeds >4 m s^{-1} compared to strong wind events (>11 m s^{-1}). The frequency of wind speeds between 5 and 10 m s^{-1} during the four years of data considered in this study represented 59% of the recorded wind events >4 m s^{-1}, whereas extreme wind events between 11 and 20 m s^{-1} represent less than 1 %. The uniform distribution of φ_v found for canopy trees in the MF habitat is evidence that the position and size of neighbours is less relevant than winds to the direction of crown displacement at higher environmental stress sites, as opposed for trees growing in the IB habitat. While crown displacement, for IB *A. germinans* trees growing below the canopy was best explained only through the sole effect of asymmetric neighbourhoods, suggesting that below canopy trees at lower salinities are well protected from wind dynamic loading, and that canopy trees in lower salinities are protected from winds by dense, bigger and crowded crowns, as found by MacFarlane & Kane (2017), who discuss that the reduced mechanical stability of spindly stems can be sustained by the protection from wind provided by neighbouring trees.

Additionally, the greater D_b for trees between 5 and 10 m for trees below the canopy, suggests that crown biomass develops towards light-available spaces while crowns above the canopy, which have gained space, are more symmetric. But D_b can also be an indicator of species light demand attributes. As described by Longuetaud et al., (2013), lower crown asymmetry is related to species shade tolerance, for this study, the lowest D_b values were found for *R. mangle,* a shade tolerant species, while *A. germinans* and *L. racemosa* (both with significantly greater D_b), are recognized as light demanding species, (Farnsworth & Ellison, 1996; Imbert, Rousteau, & Scherrer, 2000; Krauss & Allen, 2003). These species-specific traits

417 can also explain the low contribution of crown asymmetry and displacement to reducing crown
418 overlap for the plots IB2 and IB3, which have no great difference in salinity values, but have a
419 contrasting species composition. Plot IB2 was dominated by *R. mangle* trees, and in it, the
420 reduction on crown overlap attributable to crown displacement and asymmetry was only 11%, as
421 compared to the reduction observed for *A. germinans* dominated plot IB3, where active crown
422 movements accounted for 39% of canopy overlap reduction. The species *A. germinans* is one of
423 the most salt-tolerant mangrove species, and this can be explained by its multiple plastic traits.
424 Possessing a secondary successive cambia, combined with reduced vessel length and density, is
425 suggested to contribute to a safer hydraulic architecture, allowing a fast recovery from
426 embolisms (Angeles, López-Portillo, & Ortega-Escalona, 2002; Schmitz, Verheyden, Kairo,
427 Beeckman, & Koedam, 2007). These attributes could aid in a faster recovery from mechanical
428 damage to canopies, and contribute to the dominance of this species in forest stands.

429 Under the scenario of environmental change and sea-level rise, understanding tree
430 responses to increased storm frequency and intensity becomes relevant to predict changes in
431 ecosystem function. Many studies have shown that saline stress in mangrove forests decreases
432 growth and photosynthetic rates (Ball, 1988; Nguyen et al., 2015), and increased storm
433 frequency and intensity could also contribute to reduced growth rates (Rudnicki et al., 2004,
434 2001), limiting the time for crown recovery. This can potentially lead to reduced productivity
435 and efficiency in coastal protection, as canopies open and lose the ability to damp wind forces.
436 Further research is needed to understand the direction of changes in ecosystem function to
437 develop adaptation strategies for environmental change.
438

Conclusions

While active crown movements represent a fundamental strategy towards optimal light foraging, this is modulated by the reduced plant growth, smaller crowns and more open canopies in habitats with higher saline stress, exposing trees to increasing the effect of wind pressure as the main driver of crown asymmetry.

Our study shows that the mudflat habitat, subject to higher saline stress is more susceptible to wind dynamic loading, and this could lead to further degradation and loss with increasing storm frequency and intensity.

Our results support the hypothesis that ecosystems are influenced by directional variables that drive population and community dynamics, and should serve as a platform to better predict changes in forest structure and ecosystem function. This is relevant not only when considering mangrove ecosystem resilience, but also to terrestrial forests that are or will eventually be affected by substantial environmental change.

Authors' contributions

A.V., U.B. and A.P. conceived the project idea. A.V. and A.L. led data collection and data base management. A.V., U.G., R.G. and J.L.P. designed the analyses and analysed the data. A.V. led the manuscript writing and all co-authors contributed to editing the drafts and gave final approval for publication.

Acknowledgments

We thank Dr. Robert Schlicht for his advice on the mathematical approaches and Dr. Frank W. Ewers for his valuable comments on this study. The project was partially financed by the German Research Foundation (DFG, grant BE 1960/7-1) to UB, the Mexican National

Commission for Biodiversity (CONABIO- project HH025) to JLP, and the Mexican National Council of Research and Technology (CONACyT, Grant 232357) to AV. All co-authors declare that there are no conflicts of interest related to this paper.

Data accessibility

The wind data used for this study can be accessed freely at the National Data Buoy Center of the National Oceanic and Atmospheric Administration (NOAA) web page https://www.ndbc.noaa.gov/station_page.php?station=lmbv4

The tree parameter and soil salinity data of this publication will be uploaded at the Enlighten: Research Data http://researchdata.gla.ac.uk/

References

Aakala, T., Shimatani, K., Abe, T., Kubota, Y., & Kuuluvainen, T. (2016). Crown asymmetry in high latitude forests : disentangling the directional effects of tree competition and solar radiation. *Oikos*, *225*(September), 1035–1043. doi:10.1111/oik.02858

Agostinelli, C., & Lund, U. (2013). Circular Statistics (version 0.4-7). Retrieved from https://r-forge.r-project.org/projects/circular

Angeles, G., López-Portillo, J., & Ortega-Escalona, F. (2002). Functional anatomy of the secondary xylem of roots of the mangrove *Laguncularia racemosa* (L.) Gaertn. (Combretaceae). *Trees - Structure and Function*, *16*, 338–345. doi:10.1007/s00468-002-0171-9

Ball, M. C. (1988). Ecophysiology of mangroves. *Trees - Structure and Function*, *2*, 129–142.

Berger, U., & Hildenbrandt, H. (2000). A new approach to spatially explicit modelling of forest dynamics: spacing, ageing and neighbourhood competition of mangrove trees. *Ecological Modelling*, *132*(3), 287–302. doi:10.1016/S0304-3800(00)00298-2

Brisson, J. (2001). Neighborhood competition and crown asymmetry in *Acer saccharum*. *Canadian Journal of Forest Research*, *31*, 2151–2159. doi:10.1139/cjfr-31-12-2151

Brisson, J., & Reynolds, J. F. (1994). The effect of neighbors on root distribution in a Creosotebush (*Larrea Tridentata*) Population. *Ecology*, *75*(6), 1693–1702.

Brooker, R. W. (2006). Plant-plant interactions and environmental change. *The New Phytologist*, *171*(2), 271–84. doi:10.1111/j.1469-8137.2006.01752.x

Brüchert, F., & Gardiner, B. (2006). The effect of wind exposure on the tree aerial architecture and biomechanics of Sitka spruce (*Picea sitchensis*, Pinaceae). *American Journal of Botany*, *93*(10),

1512–1521. doi:10.3732/ajb.93.10.1512

Easterling, D. R., Evans, J. L., Groisman, P. Y., Karl, T. R., Kunkel, K. E., & Ambenje, P. (2000). Observed variability and trends in extreme climate events: A brief review. *Bulletin of the American Meteorological Society*, *81*(3), 417–425. doi:10.1175/1520-0477(2000)081<0417:OVATIE>2.3.CO;2

Emery, N., Ewanchuk, P., & Bertness, M. D. (2001). Competition and salt-marsh plant zonation : Stress tolerators may be dominant competitors. *Ecology*, *82*(9), 2471–2485.

Farnsworth, E. J., & Ellison, A. M. (1996). Sun-shade adaptability of the red mangrove, *Rhizophora mangle* (Rhizophoraceae): changes through ontogeny at several levels of biological organization. *American Journal of Botany*, *83*, 1131–1143.

Holtmeier, F.-K., & Broll, G. (2010). Wind as an ecological agent at treelines in North America, the Alps and the European Subarctic. *Physical Geography*, *31*(3), 203–233. doi:10.2747/0272-3646.31.3.203

Imbert, D., Rousteau, A., & Scherrer, P. (2000). Ecology of mangrove growth and recovery in the Lesser Antilles: State of knowledge and basis for restoration projects. *Restoration Ecology*, *8*(3), 230–236. doi:10.1046/j.1526-100x.2000.80034.x

James, K. R., Haritos, N., & Ades, P. K. (2006). Mechanical stability of trees under dynamic loads. *American Journal of Botany*, *93*(10), 1522–1530. doi:10.3732/ajb.93.10.1522

Jucker, T., Bouriaud, O., & Coomes, D. A. (2015). Crown plasticity enables trees to optimize canopy packing in mixed-species forests. *Functional Ecology*, *29*(8), 1078–1086. doi:10.1111/1365-2435.12428

Krauss, K. W., & Allen, J. a. (2003). Influences of salinity and shade on seedling photosynthesis and growth of two mangrove species, *Rhizophora mangle* and *Bruguiera sexangula*, introduced to Hawaii. *Aquatic Botany*, *77*(4), 311–324. doi:10.1016/j.aquabot.2003.08.004

Krauss, K. W., McKee, K. L., Lovelock, C. E., Cahoon, D. R., Saintilan, N., Reef, R., & Chen, L. (2014). How mangrove forests adjust to rising sea level. *The New Phytologist*, *202*, 19–34. doi:10.1111/nph.12605

Longuetaud, F., Piboule, A., Wernsdörfer, H., & Collet, C. (2013). Crown plasticity reduces inter-tree competition in a mixed broadleaved forest. *European Journal of Forest Research*, *132*(4), 621–634. doi:10.1007/s10342-013-0699-9

Longuetaud, F., Seifert, T., Leban, J.-M., & Pretzsch, H. (2008). Analysis of long-term dynamics of crowns of sessile oaks at the stand level by means of spatial statistics. *Forest Ecology and Management*, *255*(5–6), 2007–2019. doi:10.1016/j.foreco.2008.01.003

MacFarlane, D. W., & Kane, B. (2017). Neighbour effects on tree architecture: functional trade-offs balancing crown competitiveness with wind resistance. *Functional Ecology*, *31*(8), 1624–1636. doi:10.1111/1365-2435.12865

Matthews, P. (2000). *Vector calculus* (Corrected). London: Springer-Verlag.

McKee, K. L., Mendelssohn, I. A., & Hester, M. W. (1988). Reexamination of Pore water sulfide concentrations and redox potentials near the aerial roots of *Rhizophora mangle* and *Avicennia germinans*. *American Journal of Botany*, *75*(9), 1352–1359. doi:10.2307/2444458

Méndez-Alonzo, R., Hernández-Trejo, H., & López-Portillo, J. A. (2012). Salinity constrains size inequality and allometry in two contrasting mangrove habitats in the Gulf of Mexico. *Journal of Tropical Ecology*, *28*(2), 171–179. doi:10.1017/S0266467412000016

Méndez-Alonzo, R., Pineda-García, F., Paz, H., Rosell, J. a., & Olson, M. E. (2012). Leaf phenology is associated with soil water availability and xylem traits in a tropical dry forest. *Trees - Structure and Function*. doi:10.1007/s00468-012-0829-x

Moreno-Casasola, P., López Rosas, H., Infante Mata, D., Peralta, L. A., Travieso-Bello, A. C., & Warner, B. G. (2009). Environmental and anthropogenic factors associated with coastal wetland differentiation in La Mancha, Veracruz, Mexico. *Plant Ecology*, *200*, 37–52. doi:10. 1007/sl 1258-008-9400-7

Naidoo, G. (2009). Differential effects of nitrogen and phosphorus enrichment on growth of dwarf *Avicennia marina* mangroves. *Aquatic Botany*, *90*(2), 184–190. doi:10.1016/j.aquabot.2008.10.001

Nguyen, H. T., Stanton, D. E., Schmitz, N., Farquhar, G. D., & Ball, M. C. (2015). Growth responses of the mangrove *Avicennia marina* to salinity: development and function of shoot hydraulic systems require saline conditions. *Annals of Botany*, *115*, 397–407. doi:10.1093/aob/mcu257

Nicoll, B., & Ray, D. (1996). Adaptive growth of tree root systems in response to wind action and site conditions. *Tree Physiology*, *16*(January), 891–898.

NOAA. (2016). Constinuous wind data, LMBV4 station - La Mancha beach, Mexico. *National Data Buoy Centrer. National Oceanic and Atmospheric Administration*. https://www.ndbc.noaa.gov/station_page.php?station=lmbv4

Pewsey, A., Neuhäuser, M., & Ruxton, G. D. (2013). *Circular statistics in R* (First). Oxford, UK: Oxford University Press.

Psuty, N. P., Martínez, M. L., López-Portillo, J., Silveira, T. M., García-Franco, J. G., & Rodríguez, N. A. (2009). Interaction of alongshore sediment transport and habitat conditions at laguna La Mancha, Veracruz, Mexico. *Journal of Coastal Conservation*, *13*(2), 77–87. doi:10.1007/s11852-009-0060-0

R Core Team. (2015). R: A language and environment for statistical computing. R Foundation for Statistical Computing. Vienna, Austria, Vienna, Austria. Retrieved from http://www.r-project.org/

Robert, E. M. R., Koedam, N., Beeckman, H., & Schmitz, N. (2009). A safe hydraulic architecture as wood anatomical explanation for the difference in distribution of the mangroves *Avicennia* and *Rhizophora*. *Functional Ecology*, *23*(4), 649–657. doi:10.1111/j.1365-2435.2009.01551.x

Rudnicki, M., Silins, U., & Lieffers, V. J. (2004). Crown cover is correlated with relative density, tree slenderness, and tree height in Lodgepole Pine, *50*(3).

Rudnicki, M., Silins, U., Lieffers, V. J., & Josi, G. (2001). Measure of simultaneous tree sways and estimation of crown interactions among a group of trees. *Trees - Structure and Function*, *15*(2), 83–90. doi:10.1007/s004680000080

Schmitz, N., Verheyden, A., Kairo, J. G., Beeckman, H., & Koedam, N. (2007). Successive cambia development in *Avicennia marina* (Forssk.) Vierh. is not climatically driven in the seasonal climate at Gazi Bay, Kenya. *Dendrochronologia*, *25*(2), 87–96. doi:10.1016/j.dendro.2006.08.001

Schöb, C., Armas, C., Guler, M., Prieto, I., & Pugnaire, F. I. (2013). Variability in functional traits mediates plant interactions along stress gradients. *Journal of Ecology*, *101*(3), 753–762.

572 doi:10.1111/1365-2745.12062

573 Schröter, M., Härdtle, W., & Oheimb, G. (2011). Crown plasticity and neighborhood interactions of
574 European beech (*Fagus sylvatica* L.) in an old-growth forest. *European Journal of Forest Research*,
575 *131*(3), 787–798. doi:10.1007/s10342-011-0552-y

576 Telewski, F. W. (2006). A unified hypothesis of mechanoperception in plants. *American Journal of*
577 *Botany*, *93*(10), 1466–1476. doi:10.3732/ajb.93.10.1466

578 Telewski, F. W., & Jaffe, M. J. (1986). Thigmomorphogenesis: Field and laboratory studies of *Abies*
579 *fraseri* in response to wind or mechanical perturbation. *Physiologia Plantarum*, *66*(2), 211–218.
580 doi:10.1111/j.1399-3054.1986.tb02411.x

581 Tilman, D. (1988). *Plant strategies and the dynamics and fuction of plant communities*. New Jersey:
582 Princeton Uinversity Press.

583 Tilman, D. (1990). Mechanisms of plant competition for nutrients: the elements of a directive theory of
584 competition. In J. Grace & D. Tilman (Eds.), *Perspectives on plant competition* (pp. 117–141). New
585 York, USA: Academic press.

586 Uria-Diez, J., & Pommerening, A. (2017). Crown plasticity in Scots pine (*Pinus sylvestris* L.) as a
587 strategy of adaptation to competition and environmental factors. *Ecological Modelling*, *356*, 117–
588 126. doi:10.1016/j.ecolmodel.2017.03.018

589 Vacchiano, G., Castagneri, D., Meloni, F., Lingua, E., & Motta, R. (2011). Point pattern analyisis of
590 crown-to-crown interactions in mountain forests. *Procedia Environmental Sicences*, *7*(0), 269–274.
591 doi:10.1016/j.proenv.2011.07.047

592 Vovides, A. G., Berger, U., & López-Portillo J. (2018). Data from: Change in drivers of mangrove crown
593 displacement along a salinity stress gradient. *Enlighten repository University of Glasgow*

594 Vovides, A. G., Vogt, J., Kollert, A., Berger, U., Grueters, U., Peters, R., … López-Portillo, J. (2014).
595 Morphological plasticity in mangrove trees: salinity-related changes in the allometry of *Avicennia*
596 *germinans*. *Trees - Structure and Function*, *28*, 1413–1425. doi:10.1007/s00468-014-1044-8

597 Wolf, C., Field, B., & Berry, J. A. (2011). Neighborhood competition and crown asymmetry in *Acer*
598 *saccharum*. *Ecological Society of America*, *21*(5), 1546–1556.

599 Woodroffe, C. D. (1990). The impact of sea-level rise on mangrove shorelines. *Progress in Physical*
600 *Geography*, *14*(4), 483–520. doi:10.1177/030913339001400404

601

602 Table 1. Basal area and species relative density and dominance organized by habitat and salinity. Values of salinity are average (± standard
603 error). *N* represent total number of trees in the stand and $N(n\ a_i)$ represents the number of focal trees with neighbours fully contained within the
604 plot. *Ag* stands for *A. germinans*, Lr = *Laguncularia racemosa*, *Rm* = *Rhizophora mangle*.

Site	Salinity (ppt)	Basal area ($m^2\ ha^{-1}$)			Relative density (%)			Relative dominance (%)			$N(n\ a_i)$
		Ag	*Lr*	*Rm*	*Ag*	*Lr*	*Rm*	*Ag*	*Lr*	*Rm*	
IB1	4.6 (0.54)	20	32	-	70	30	-	38	62	-	58 (20)
IB3	25.4 (0.5)	19	14	3.5	39	23	38	50	40	10	123 (46)
IB2	26.8 (0.09)	17	11	15	23	15	62	39	25	36	58 (25)
IB6	37.5 (0.96)	28	0.01	1.5	54	2	44	95	0.05	4.95	54 (28)
IB5	42.0 (2.22)	29	-	1.0	62	-	38	97	-	3.	47 (19)
IB4	44.3 (0.92)	34	-	3.5	60	-	40	90	-	10	81 (34)
MF5	39.2 (0.60)	46	1.0	0.6	70	2	28	97	2	1	76 (23)
MF2	43.5 (1.5)	27	-	0.2	83		17	99	-	1	28 (13)
MF3	48.0 (2.27)	56	-	0.3	92	-	8	99.5	-	0.5	56 (17)
MF1	49.4 (2.11)	27	-	0.2	97	-	3	99.8	-	0.2	38 (13)
MF4	55.7 (1.5)	35	-	-	100	-	-	100	-	-	43 (19)
MF6	60.4(2.52)	56	-	-	100	-	-	100	-	-	80 (32)

605

606 Table 2. Rayleigh tests for uniformity to assess the aggregation of angles of alignment (φ^o, mean ± Confidence intervals at 95% estimated by the
607 method of maximum likelihood boot strap for a von Misses distribution at 1,000 repetitions) between vector of crown displacement (u_i) and
608 vectors of pressure with: no wind effect ($\varphi^o{}_v$), only wind effect ($\varphi^o{}_w$) and with effect of wind and neighbours ($\varphi^o{}_{nw}$), at Interdistributary Basins
609 (IB) and Mudflats (MF) for *A. germinans* and *R. mangle*, with crowns located at the canopy level (≥ 15 and ≥ 13 for IB and MF, respectively) and
610 below canopy (<15 and < 13, for IB and MF, respectively). ρ is the concentration parameter (proportion of data concentrated around the mean). N
611 indicates the number of focal trees within the analysis, * stands for significant aggregation at *= P <0.05, **= P < 0.001, and ***= $P<0.0001$.

	Avicennia germinans							*Rhizophora mangle*						
	N	$\varphi^o{}_v$		$\varphi^o{}_w$	ρ	$\varphi^o{}_{nw}$	ρ	N	$\varphi^o{}_v$	ρ	$\varphi^o{}_w$	ρ	$\varphi^o{}_{nw}$	ρ
IB														
≥ 15	40	175(22)	0.48^{***}	155(28)	0.33^{*}	173(24)	0.49^{***}	12	111(101)	0.18	210(63)	0.30	213(47)	0.49^{*}
< 15	37	168(47)	0.29^{*}	182(64)	0.13	204(85)	0.18	50	149(97.6)	0.23	205(27)	0.22^{**}	203(26)	0.40^{***}
MF														
≥ 13	40	184(62)	0.24	153(46)	0.18^{*}	171(32)	0.41^{**}							
< 13	67	205(30)	0.32^{**}	157(28)	0.21^{*}	171(22)	0.38^{***}	7	236(49)	0.58	214(92)	0.16	252(37)	0.70^{*}

Figure legends

Figure 1. Study plots in La Mancha Lagoon, Veracruz, Mexico. Six plots are in the Interdistributary basin (IB, light grey), and six in Mudflat (MF, dark grey) habitats, values close to the plot identifier are average salinity values. The wind rose shows overall wind speed events and directions, the blue arrow depicts the circular mean wind direction.

Figure 2. Vectors used to estimate crown displacement in relation to neighbours. (a) the open circle is the stem base positions of the focal tree (S_i) , filled circles are neighbours (S_j), × represent the crowns centroids (G_i) of each tree. Dashed arrows are the vectors S_i and S_j, the solid grey arrow is the vector of crown displacement (u_i), and the solid black arrow is the vector of neighbourhood asymmetry (v_i). (b) Shows the dot product (a_i) of vectors u_i and v_i, used as a measure of crown displacement in the direction of v_i, and φ is the angle between the vectors to assess the direction of displacement of u_i in relation to v_i. (c) Depicts crown area overlap with the observed crown displacement, and a relative overlap (O_{crown}), Open circles are stem positions and ×, (d) is shows crown area overlap when G_i is positioned above S_i (O_{stem}), and (e) shows the overlap of symmetric crowns reconstructed from the observed tree crown areas (O_{symm}).

Figure 3. Generalized mixed effects model with a Markov chain Monte Carlo algorithm (MCMC) to evaluate the contribution of the vector of neighbourhood asymmetry to crown displacement (a_i) along a salinity gradient for *Avicennia germinans* (blue solid line and open circles), *Laguncularia racemosa* (green discontinuous line and open triangles) and *Rhizophora mangle* (red dashed line and open squares).

635

636

637 Figure 4. Generalised mixed effects model with MCMC posterior density curves for the
638 alignment of neighbourhood asymmetry (a_i) showing greater avoidance of neighbors for *A.*
639 *germinans* (blue curve centred on negative values), while *R. mangle* (red) and *Laguncularia*
640 *racemosa* (green) concentrate around positive values of a_i.

641

642 Figure 5. Crown displacement direction for trees at the canopy level (green circles) and below
643 the canopy (blue circles), polygons indicate mean direction of crown displacement ± 95%
644 confidence intervals estimated with a maximum likelihood boot strap for a von Misses
645 distribution for trees at the canopy level (green) and below the canopy (blue). Asterisks (*)
646 indicate significant concentration parameter as per Rayleigh's test for circular data.

647

648 Figure 6. Circular representation of angles of alignment (φ) between vector of crown
649 displacement and vector of pressure. φ_v (left column) is the angle between vector of crown
650 displacement and neighbourhood asymmetry, φ_{nw} is the angle between vectors of crown
651 displacement and the synthesised effect of wind and neighbours (right column) for: *A. germinans*
652 in Interdistributary Basins (a-b), and *R. mangle* (c-d), and in Mudflat habitats (e-f, and g-h, for *A.*
653 *germinans* and *R. mangle* respectively). Polygons indicate mean angles φ ± 95% confidence
654 intervals estimated with a maximum likelihood boot strap for a von Misses distribution for
655 canopy (green polygons) and below the canopy trees (blue shaded). The length of the polygon
656 represents the concentration parameter (ρ), and asterisks (*) indicate significant aggregation of
657 data towards a given angle.

658

659 Figure 7. Additive mixed effects model showing differences on crown asymmetry (D_b) of three
660 tree species growing at the Interdistributary basins (IB) and the Mudflat habitats (MF). Tree
661 height was used as smoothing term, habitat as random effects, and species and salinity as fixed
662 effects.

663

664 Figure 8. Generalised linear mixed effects model correlating the reduction percentage on crown
665 projected area overlap (ΔO) due to crown displacement along a salinity gradient. Red circles
666 show changes related only to crown displacement ($\Delta O_{stem-crown}$) and blue triangles depict
667 changes when simulating perfectly symmetric crowns ($\Delta O_{symm-crown}$) in Interdistributary
668 basins (filled symbols) and Mudflats (open symbols).

669

670

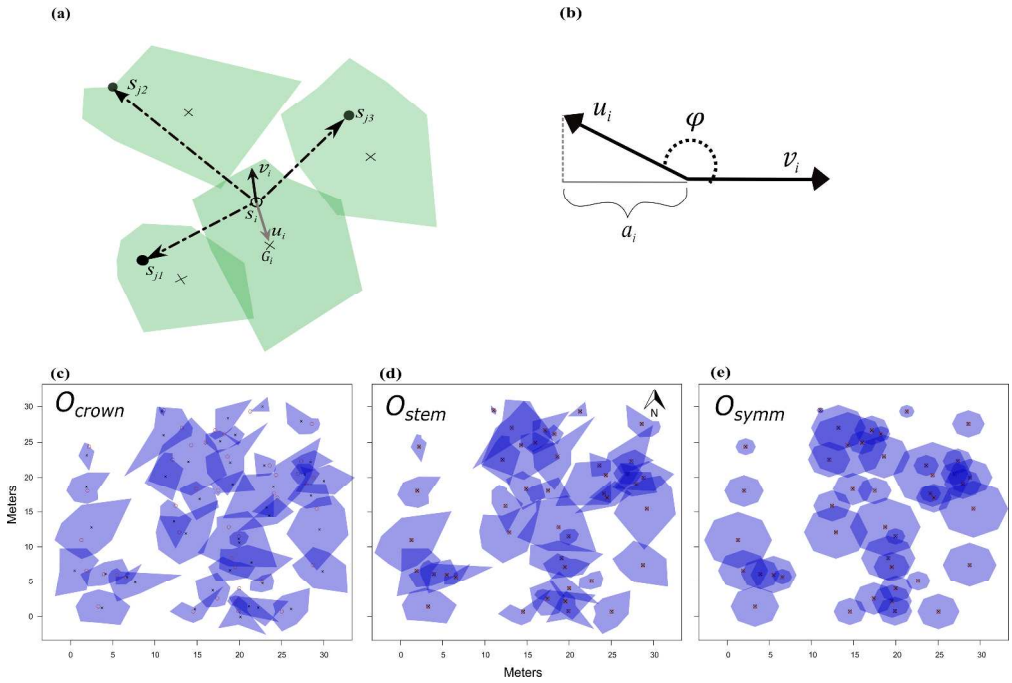

Figure 2. Vectors used to estimate crown displacement in relation to neighbours. (a) the open circle is the stem base positions of the focal tree (S_i) , filled circles are neighbours (S_i), × represent the crowns centroids (G_i) of each tree. Dashed arrows are the vectors S_i and S_j, the solid grey arrow is the vector of crown displacement (u_i), and the solid black arrow is the vector of neighbourhood asymmetry (v_i). (b) Shows the dot product (a_i) of vectors u_i and v_i, used as a measure of crown displacement in the direction of v_i, and φ is the angle between the vectors to assess the direction of displacement of u_i in relation to v_i. (c) Depicts crown area overlap with the observed crown displacement, and a relative overlap (O_{crown}), Open circles are stem positions and ×, (d) is shows crown area overlap when G_i is positioned above S_i (O_{stem}), and (e) shows the overlap of symmetric crowns reconstructed from the observed tree crown areas (O_{symm}).

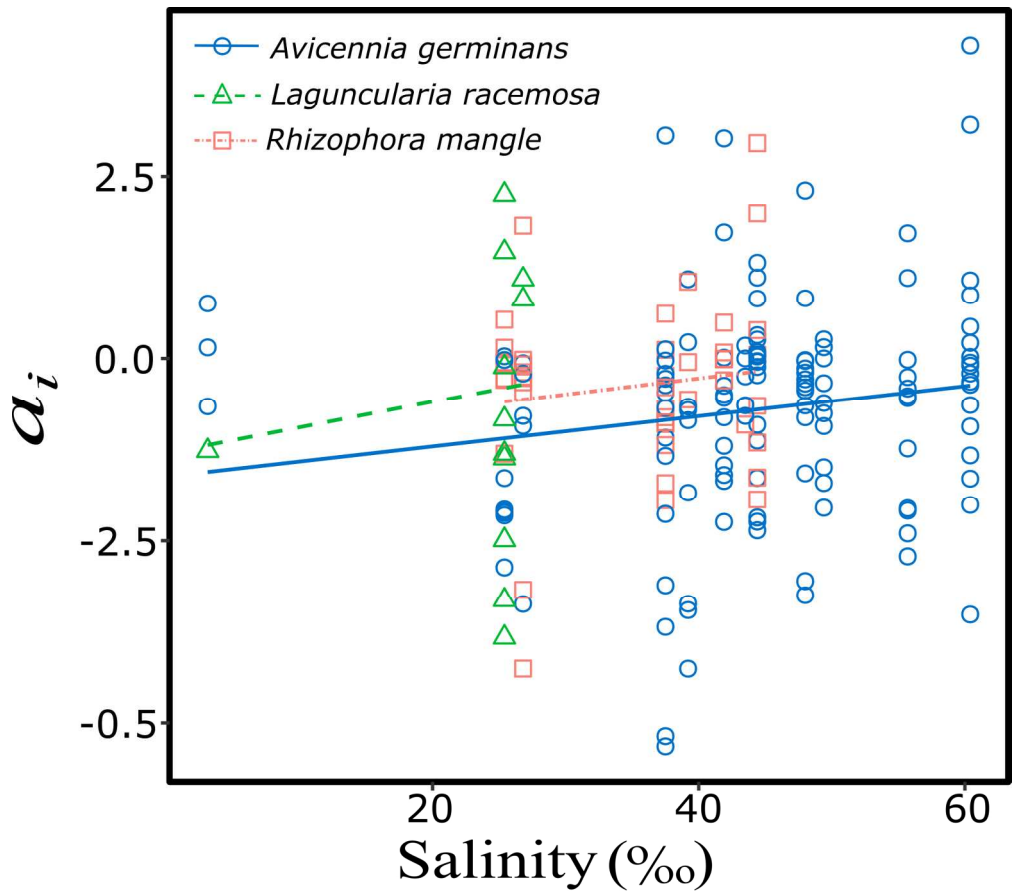

Figure 3. Generalized mixed effects model with a Markov chain Monte Carlo algorithm (MCMC) to evaluate the contribution of the vector of neighbourhood asymmetry to crown displacement (a_i) along a salinity gradient for *Avicennia germinans* (blue solid line and open circles), *Laguncularia racemosa* (green discontinuous line and open triangles) and *Rhizophora mangle* (red dashed line and open squares).

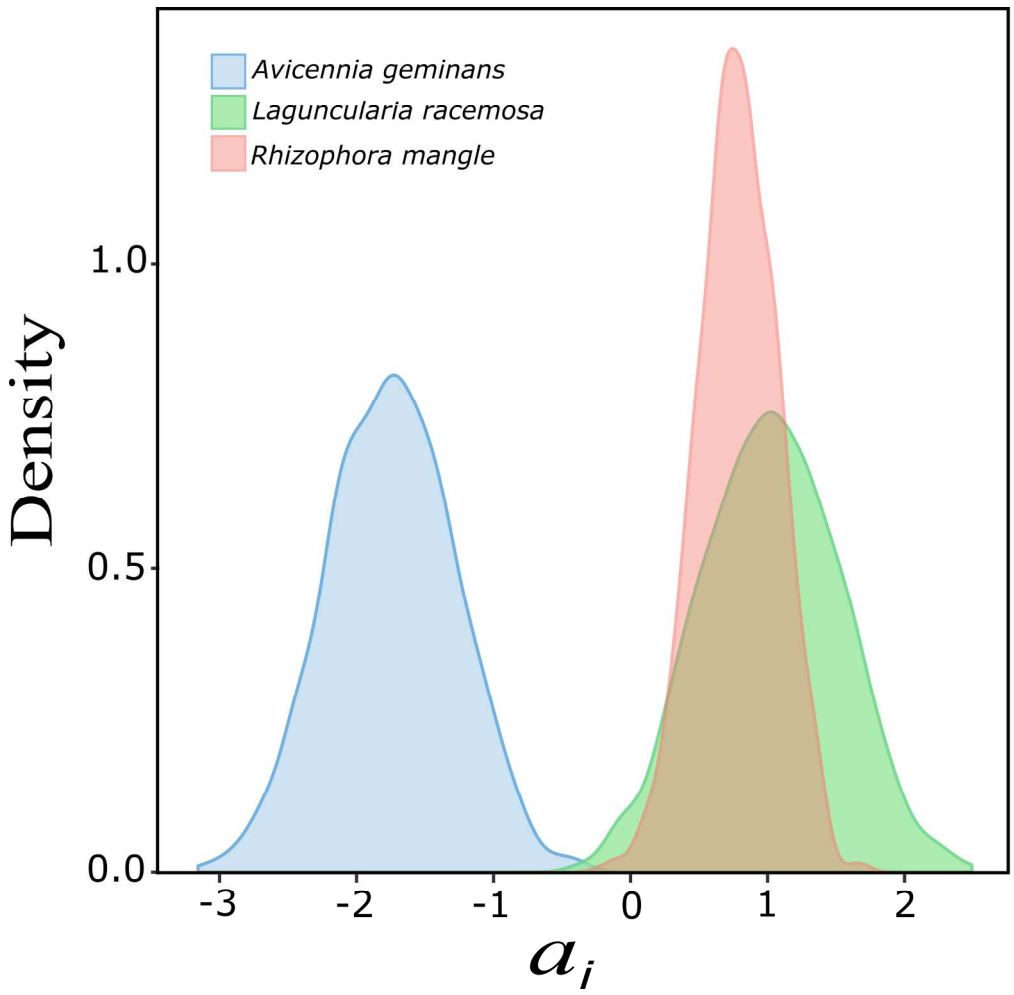

Figure 4. Generalised mixed effects model with MCMC posterior density curves for the alignment of neighbourhood asymmetry (a_i) showing greater avoidance of neighbors for *A. germinans* (blue curve centred on negative values), while *R. mangle* (red) and *Laguncularia racemosa* (green) concentrate around positive values of a_i.

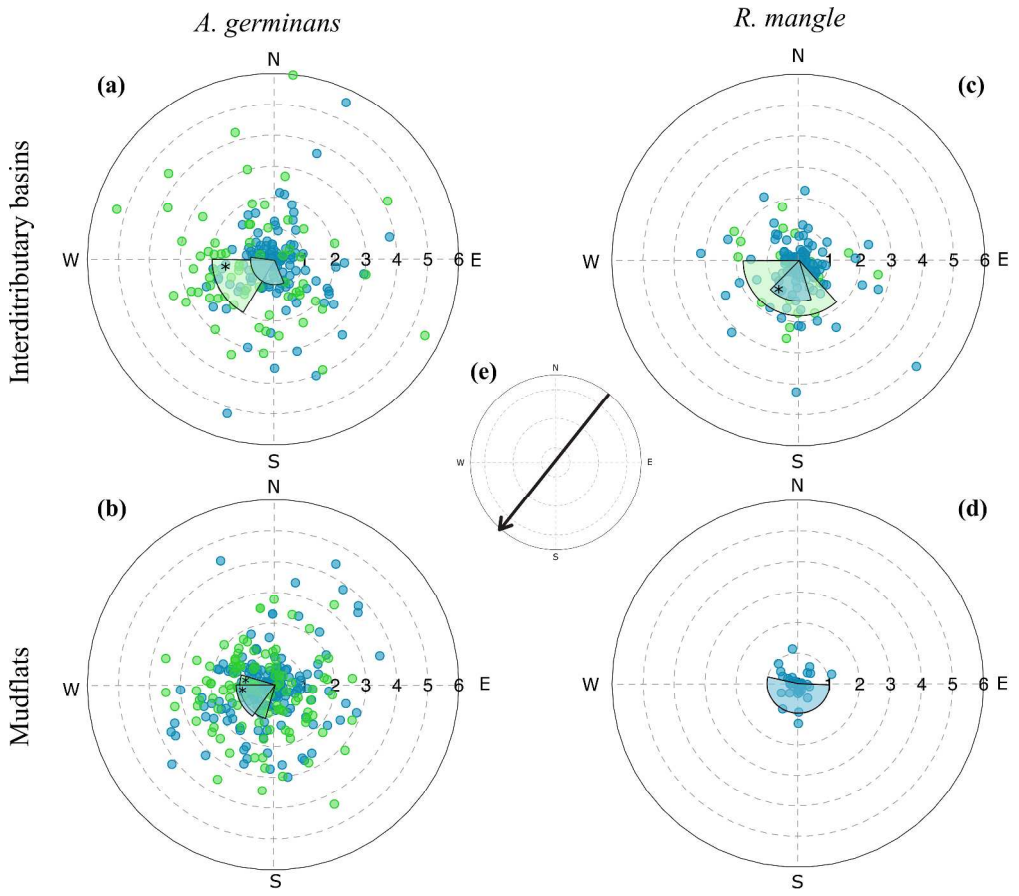

Figure 5. Crown displacement direction for trees at the canopy level (green circles) and below the canopy (blue circles), polygons indicate mean direction of crown displacement ± 95% confidence intervals estimated with a maximum likelihood boot strap for a von Misses distribution for trees at the canopy level (green) and below the canopy (blue). Asterisks (*) indicate significant concentration parameter as per Rayleigh's test for circular data.

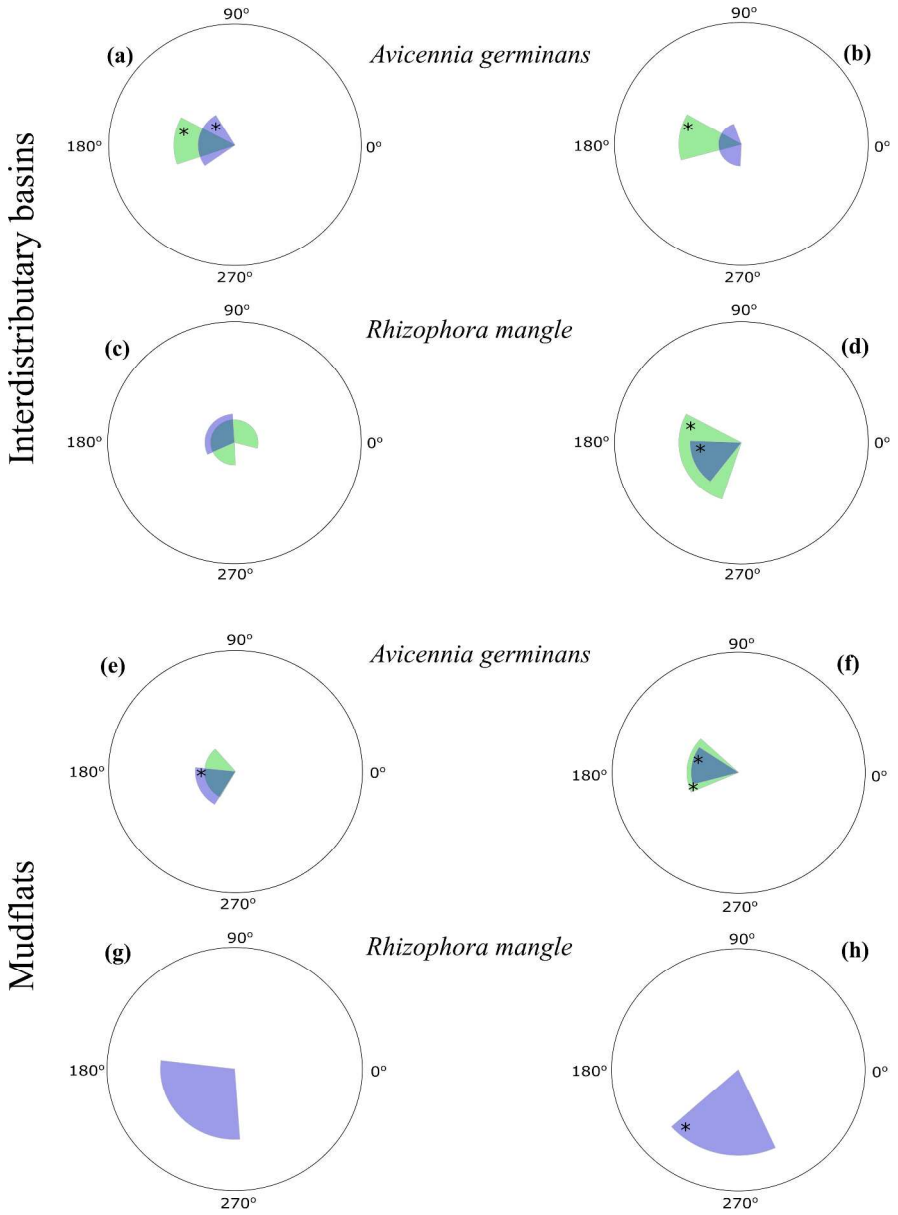

Figure 6. Circular representation of angles of alignment (φ) between vector of crown displacement and vector of pressure. φ_v (left column) is the angle between vector of crown displacement and neighbourhood asymmetry, φ_{nw} is the angle between vectors of crown displacement and the synthesised effect of wind and neighbours (right column) for: *A. germinans* in Interdistributary Basins (a-b), and *R. mangle* (c-d), and in Mudflat habitats (e-f, and g-h, for *A. germinans* and *R. mangle* respectively). Polygons indicate mean angles φ ± 95% confidence intervals estimated with a maximum likelihood boot strap for a von Misses distribution for canopy (green polygons) and below the canopy trees (blue shaded). The length of the polygon represents the concentration parameter (ρ), and asterisks (*) indicate significant aggregation of data towards a given angle.

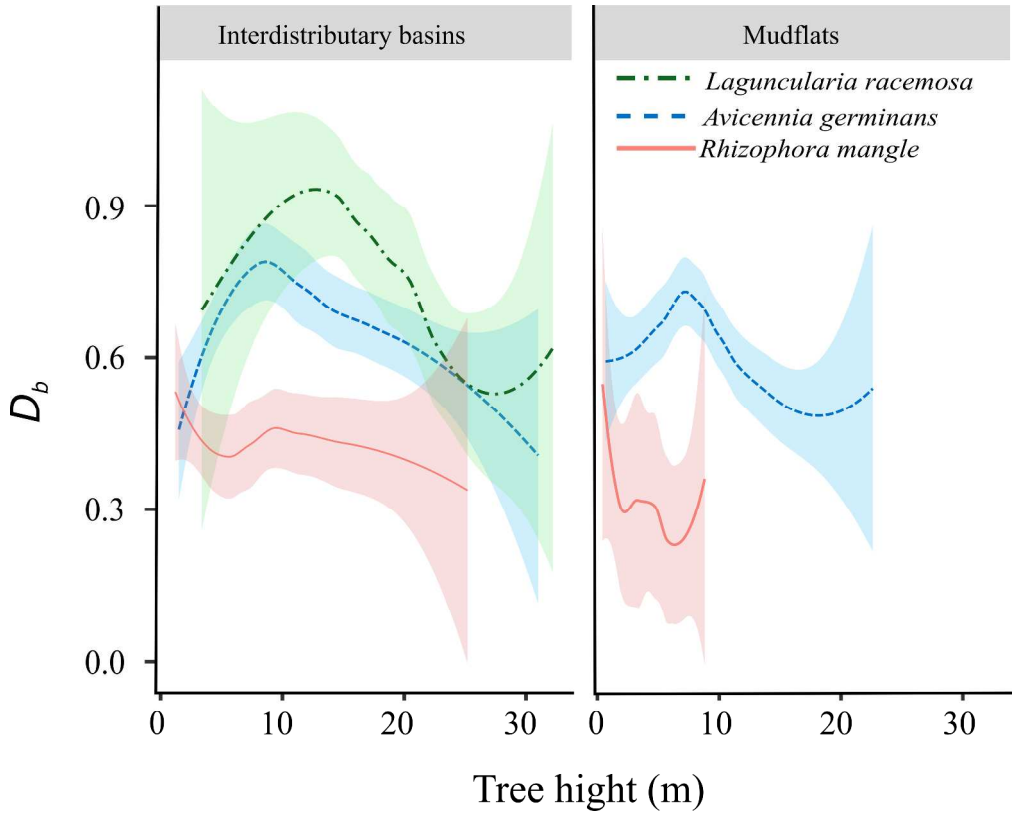

Figure 7. Additive mixed effects model showing differences on crown asymmetry (D_b) of three tree species growing at the Interdistributary basins (IB) and the Mudflat habitats (MF). Tree height was used as smoothing term, habitat as random effects, and species and salinity as fixed effects.

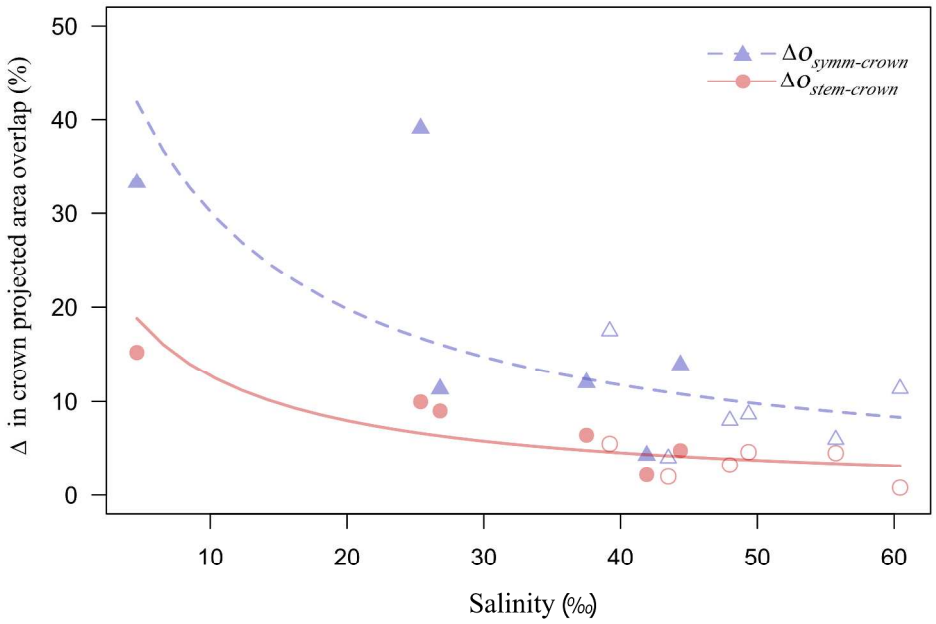

Figure 8. Generalised linear mixed effects model correlating the reduction percentage on crown projected area overlap (ΔO) due to crown displacement along a salinity gradient. Red circles show changes related only to crown displacement ($\Delta O_{stem\text{-}crown}$) and blue triangles depict changes when simulating perfectly symmetric crowns ($\Delta O_{symm\text{-}crown}$) in Interdistributary basins (filled symbols) and Mudflats (open symbols).

Appendix S1. Computation of symmetric octagons from crown-projected areas measured in the field

To quantify crown-projected area overlap assuming absolute symmetry (no crown asymmetry nor displacement), we used the measured crown areas of each tree to compute regular octagons following(Goetze, 1998), and further mapped them in the plots, locating the centroid of the octagon at each tree's stem position.

Since in a regular octagon all circumradii (the distance between the centroid an any vertex of the octagon) have the same length (Fig. 1), to compute regular octagons, we substituted the length of the eight measured crown radii with the length of the circumradius (R) computed for each crown as:

$$R = \frac{1}{2}\sqrt{4 + 2\sqrt{2}} \cdot ed$$

Where ed is the length of an edge of the octagon (Fig. 1), calculated by dividing the octagon's perimeter (P) by eight ($ed = \frac{P}{8}$). For each crown P was computed using crown area (A) as follows:

$$P = \sqrt{\frac{32 \cdot A}{1 + \sqrt{2}}}$$

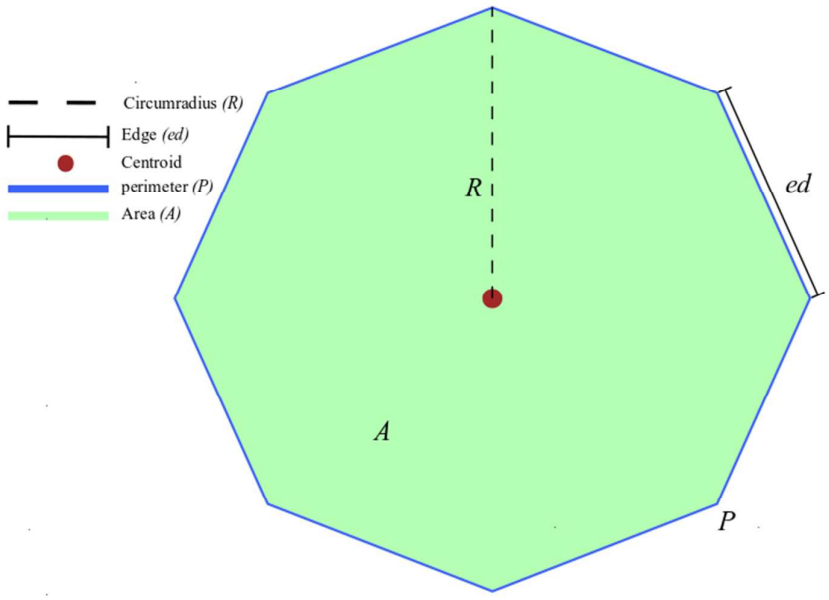

Figure 1. Components of a symmetric octagon used to reshape crown-projected areas from the observed asymmetric polygons to a symmetric octagon. The blue line is the perimeter (P) of the octagon, which divided by eight, returns the length of each octagon edge (ed). The green colour represents the area (A), brown is the centroid of the octagon, and the dotted line is the circumradius.

Crown-projected areas were then mapped with: 1) their observed displacement and asymmetry (Fig. 2A), 2) assuming no crown displacement, by centring crown polygons on stem position (Fig 2B), and 3) by simulating symmetric crowns with no displacement (Fig. 2C). Maps were then analysed in GIMP V2.8 image analysis package to quantify for CPA overlap under the three scenarios.

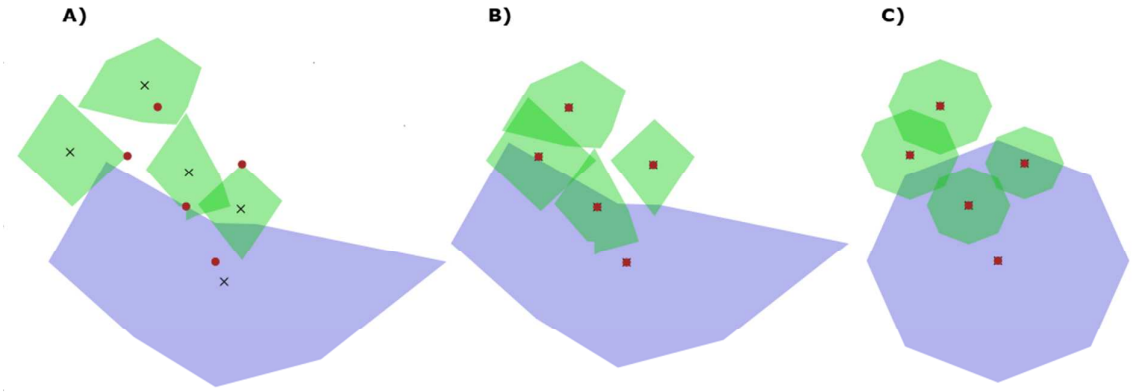

Figure 2 Crown projected areas with: **A)** their observed crown displacement, **B)** the observed asymmetry, but matching crown centroid (×) with stem position (brown circle), assuming no crown displacement occurred and, **C)** simulating absolute symmetry (regular crowns centred on stem position).

Reference

Goetze, H. (1998). *Castel del Monte: Geometric Marvel of the Middle Ages*. Munich, Germany: Prestel.